Electroanalytical Chemistry and Interfacial Electrochemistry, 44 (1973) 169–187

CONVOLUTIVE POTENTIAL SWEEP VOLTAMMETRY

I. INTRODUCTION

J. C. IMBEAUX and J. M. SAVÉANT
Laboratoire d'Electrochimie, Université de Paris VII, 2 place Jussieu, 75-Paris (5e) (France)
(Received 20th November 1972)

In a previous article[1] we have suggested that a valuable improvement in the practice of linear sweep voltammetry (LSV) would consist of computing convolution integrals of the type:

$$I = \frac{1}{\pi^{\frac{1}{2}}} \int_0^t \frac{i(\upsilon)}{(t-\upsilon)^{\frac{1}{2}}} \, d\upsilon$$

directly from the experimental current–time curves (i–t), (see pp. 176 and 177 in ref. 1). So, quantities proportional to the diffusing reactant concentrations at the electrode surface would be directly available from experimental data. It was noted that it would be possible to do this without unreasonable tedium by converting first the analog output signal into a digital form and then calculating the convolution integral I by means of a computer.

The main applications of such a modification of the usual data processing in LSV, which will be termed Convolution Potential Sweep Voltammetry (CPSV) in the following, were considered mainly in the field of mechanism analysis. They were thought to arise from the following features:

(*a*) the possibility of using all the information contained in a single current–time (or potential) curve instead of only that involved in the peak values. So, the accuracy in mechanism diagnosis and rate constant determination is increased. A further improvement in this direction is obtained by using time-averaging techniques to which the digitalized form of the output signal lends itself readily.

(*b*) the elimination of a severe limitation of LSV as regards the study of potential dependent phenomena, that is, the necessity of an *a priori* knowledge of the form of the kinetic law in order to compare a given model to the experimental data. This arises from the availability of experimental reactant concentrations at the electrode surface. Also the analysis of a reaction mechanism involving fast and irreversible homogeneous chemical steps ("pure kinetic" conditions) is greatly facilitated since it generally involves simple mathematical relationships between the reactant concentrations at the electrode and the current.

Recently Oldham and Grenness[2,3] have proposed, under the heading "semi-integral electroanalysis" a similar transformation of the current–time curve in the case of a diffusion controlled charge transfer with reference to analytical applications rather than to kinetic analysis of mechanisms.

The purpose of the present paper is to describe in more detail than we did previously the possibilities of CPSV in the field of mechanism analysis and to present some preliminary experiments testing the practical applicability of the method. The basic types of reaction schemes involving slow charge transfers and/or fast irreversible chemical reactions will be exemplified in forthcoming papers. Discussions are based on reduction processes. Transposition to oxidation is immediate.

DIFFUSION CONTROLLED CHARGE TRANSFER

Single wave. Linear diffusion

Consider the following simple reaction scheme

$$A + n\,e \rightleftharpoons B \quad \text{(standard potential } E^0\text{)}$$

where the forward and backward rates are assumed to be so large that the Nernst law applies and the current is controlled by diffusion along the entire wave. If diffusion is assumed to be linear and semi-infinite, the concentrations $C_A(x, t)$ and $C_B(x, t)$ of the reacting species are solutions of the well known system:

$$\partial C_A/\partial t = D_A\,\partial^2 C_A/\partial x^2$$
$$\partial C_B/\partial t = D_B\,\partial^2 C_B/\partial x^2$$

$t=0$, $x \geqslant 0$, and $x=\infty$, $t \geqslant 0$:

$$C_A = C^0 \quad \text{(initial concentration)}, \quad C_B = 0 \tag{1}$$

$x=0$, $t \geqslant 0$:

$$D_A\,\partial C_A/\partial x = -D_B\,\partial C_B/\partial x \qquad (D_A, D_B = \text{diffusion coefficients})$$
$$C_A = C_B \exp(nF/RT)(E-E^0) \qquad (E = \text{electrode potential})$$

The observed quantity is the current:

$$i = nFSD_A(\partial C_A/\partial x)_0$$

(S=electrode surface area. The subscript 0 indicates that the considered space-dependent quantity is taken at the electrode surface).

Defining:

$$\tau = t/\theta, \quad y = x/(D_A\,\theta)^{\frac{1}{2}}, \quad a = C_A/C^0, \quad b = C_B/C^0$$

where θ is an arbitrary fixed value of time.

$$\Psi = i\theta^{\frac{1}{2}}/nFSC^0 D_A^{\frac{1}{2}} \tag{2}$$

The above system becomes:

$$\partial a/\partial\tau = \partial^2 a/\partial y^2 \tag{3}$$

$$\partial b/\partial\tau = d\,\partial^2 b/\partial y^2 \quad (d = D_B/D_A) \tag{4}$$

$\tau=0$, $y \geqslant 0$ and $y=\infty$, $\tau \geqslant 0$: $a=1$, $b=0$ (5)

$y=0$, $\tau \geqslant 0$: $\Psi = \partial a/\partial y = -d(\partial b/\partial y)$

$$a = b \exp(nF/RT)(E-E^0). \tag{6}$$

From integration of (3) and (4) in the Laplace space and taking (5) into account it follows that:

$$\overline{a_0} = \frac{1}{s} - \frac{\bar{\Psi}}{s^{\frac{1}{2}}} \quad \text{and} \quad \overline{b_0} = \frac{1}{d^{\frac{1}{2}}} \frac{\bar{\Psi}}{s^{\frac{1}{2}}}$$

where s is the Laplace variable and the bar indicates a Laplace transformed function.

Then,

$$a_0 + d^{\frac{1}{2}} b_0 = 1,$$

on the other hand from (6) it follows that:

$$\frac{a_0}{\exp(nF/RT)(E-E_{\frac{1}{2}})} = d^{\frac{1}{2}} b_0 = \frac{1}{1+\exp(nF/RT)(E-E_{\frac{1}{2}})}$$

$E_{\frac{1}{2}}$ being the polarographic half-wave potential defined as:

$$E_{\frac{1}{2}} = E^0 + (RT/2nF) \ln D_B/D_A).$$

Defining the dimensionless electrode potential variable as:

$$\xi = -(nF/RT)(E-E_{\frac{1}{2}}) \tag{7}$$

It follows that:

$$1 - a_0 = d^{\frac{1}{2}} b_0 = 1/\{1+\exp(-\xi)\}$$

The original of $\bar{\Psi}/s^{\frac{1}{2}}$ is the dimensionless convolution integral.

$$I\Psi = \frac{1}{\pi^{\frac{1}{2}}} \int_0^{\tau} \frac{\Psi}{(\tau-\upsilon)^{\frac{1}{2}}} \, d\upsilon$$

Then:

$$I\Psi = 1/\{1+\exp(-\xi)\}$$

The results obtained in dimensionless form are summarized in Fig. 1 where Ψ, $I\Psi$, a_0 and $d^{\frac{1}{2}} b_0$ are represented as functions of ξ. It is seen that $I\Psi$ has the

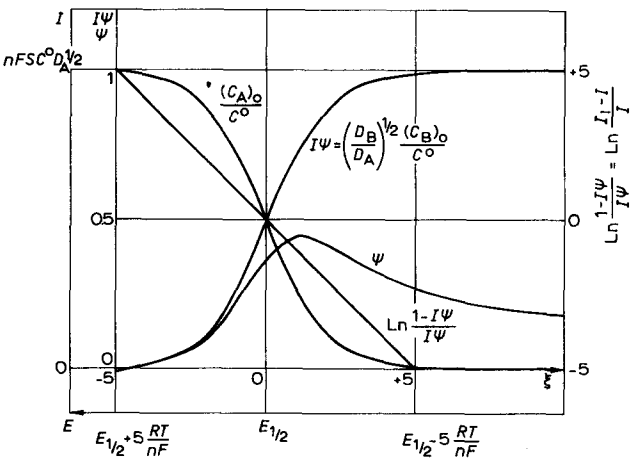

Fig. 1. Current, convoluted current, surface concentration and logarithmic analysis for pure diffusion control.

same shape as a polarogram and tends toward 1 when $\xi \to \infty$. The wave equation can be rewritten:

$$-\xi = \ln\{(1-I\Psi)/I\Psi\} \tag{8}$$

Then the logarithmic analysis of the "$I\Psi$ wave" leads to a straight line.

Turning back to dimensioned quantities:

$$I = nFSC^0 D_A^{\frac{1}{2}} I\Psi$$

and

$$E = E_{\frac{1}{2}} - (RT/nF)\xi$$

Thus the same diagram represents on Fig. 1 the function $I(E)$ as well as $I\Psi(\xi)$. The limiting value of the polarographic type curve for $E \to \infty$ is now:

$$I_l = nFSC^0 D_A^{\frac{1}{2}} \tag{9}$$

and the logarithmic analysis of the wave:

$$E = E_{\frac{1}{2}} + (RT/nF)\ln\{(I_l - I)/I\} \tag{10}$$

follows exactly the same lines as for a polarographic wave or a rotating disc electrode wave.

It is seen that:

$$(C_A)_0 = C^0 - I/nFSD_A^{\frac{1}{2}} = C^0(1 - I/I_l) \tag{11}$$

and

$$(C_B)_0 = I/nFSD_B^{\frac{1}{2}} = C^0(D_A/D_B)^{\frac{1}{2}} I/I_l \tag{12}$$

The following conclusions can thus be drawn:

(*a*) up till now, the way in which the electrode potential sweeps from the foot to the top of the polarographic wave has not been defined because it did not need to be defined. The only condition to be ensured is that the potential at the foot of the wave be such that the initial condition (3) is fulfilled with a given accuracy. Also, of course, the final potential must be cathodic enough to the half-wave potential for the plateau to be reached.

(*b*) in practice, however, the input potential signal is a definite function of time and a simple function is recommended in any case in order to define unambiguously the rate of diffusion. This will become apparent in the following study of processes that are controlled not only by diffusion but in which diffusion competes kinetically with other phenomena such as charge transfer or chemical reactions. Then the extent of the competition is modified by a variation in the diffusion rate. A convenient input signal in this connection is a linear sweeping of the electrode potential. The main factor which determines the diffusion rate is then the sweep rate.

(*c*) the dimensions of the quantity I are not those of current. I has the same dimensions as $q\,t^{-\frac{1}{2}}$, where q represents a charge and t the time.

(*d*) when sweeping the electrode potential linearly, the actual potential difference across the faradaic impedance has not exactly the same form, due to ohmic drop in the uncompensated resistance. From the arbitrary character of the input signal underlined above it can thus be seen that the procedure for ohmic drop correction will be much simpler with CPSV than with LSV.

(*e*) from the consideration of an unspecified input potential in the above discussion the conclusion also arises that when cyclic scanning of the electrode potential is performed the *I* "return" curve is exactly superimposable on the direct curve as is the current curve in polarography.

(*f*) this last feature is by no means specific of a nernstian system and is not therefore a "reversibility" test. It will be shown in the following that this behaviour is also observed for perfectly irreversible systems again as for standard polarograms. The existence of a plateau in the *I–E* curve does not necessarily result from a nernstian character. Indeed a sufficient condition to observe a plateau is, *e.g.*:

$$(C_A)_0 = C^0 - I/nFSD_A^{\frac{1}{2}} \quad \text{and} \quad (C_A)_0 \to 0 \text{ when } E \to -\infty$$

which is fulfilled when diffusion control occurs but not only in this case.

(*g*) an actual test of reversibility is provided by logarithmic analysis. It suffices to check that the resulting straight line has the right slope: RT/nF ($59.1/n$ mV at 25°C for decimal logarithms). This is a much simpler test than in CV where an accurate evaluation of reversibility requires the re-construction of the anodic curve from the extension of the cathodic one beyond the inversion point.

Successive waves

Consider *e.g.*, two successive nernstian charge transfers:

$A + ne \rightleftharpoons B$ (standard potential E_1^0)

$B + ne \rightleftharpoons C$ (standard potential E_2^0)

For simplicity, the number of electrons transferred in both steps is assumed to be the same and the diffusion coefficients to be equal.

The partial derivative equation system is now:

$$\partial C_A/\partial t = D\,\partial^2 C_A/\partial x^2$$

$$\partial C_B/\partial t = D\,\partial^2 C_B/\partial x^2$$

$$\partial C_C/\partial t = D\,\partial^2 C_C/\partial x^2$$

$$t=0,\ x \geqslant 0 \text{ and } x=\infty,\ t \geqslant 0\text{: } C_A = C^0,\ C_B = C_C = 0$$

$$x=0,\ t \geqslant 0\text{: } (\partial C_A/\partial x)+(\partial C_B/\partial x)+(\partial C_C/\partial x)=0$$

$$C_A = C_B \exp(nF/RT)(E-E_1^0), \quad C_B = C_C \exp(nF/RT)(E-E_2^0) \tag{13}$$

The current is:

$$i = nFSD\{(\partial C_A/\partial x)_0 - (\partial C_C/\partial x)_0\} = nFSD\{2(\partial C_A/\partial x)_0 + (\partial C_B/\partial x)_0\}$$

In dimensionless form:

$$\partial a/\partial \tau = \partial^2 a/\partial y^2, \quad \partial b/\partial \tau = \partial^2 b/\partial y^2, \quad \partial c/\partial \tau = \partial^2 c/\partial y^2$$

$$\tau = 0,\ y \geqslant 0 \text{ and } y=\infty,\ \tau \geqslant 0\text{: } a=1,\ b=c=0$$

$$y=0,\ \tau \geqslant 0\text{: } (\partial a/\partial y)+(\partial b/\partial y)+(\partial c/\partial y)=0$$

$$a = b \exp(nF/RT)(E-E_1^0), \quad b = c \exp(nF/RT)(E-E_2^0)$$

$$\Psi = \Psi_1 + \Psi_2, \quad \Psi_1 = (\partial a/\partial y)_0, \quad \Psi_2 = -(\partial c/\partial y)_0$$

From integration of the system it comes out that:

$$a_0 = 1 - I\Psi_1, \quad b_0 = I\Psi_1 - I\Psi_2, \quad c_0 = I\Psi_2$$

then taking (13) into account it follows that:

$$I\Psi = \frac{2 + \exp(nF/RT)(E - E_2^0)}{1 + \exp(nF/RT)(E - E_2^0) + \exp(2nF/RT)\{E - \frac{1}{2}(E_1^0 + E_2^0)\}}$$

We assume now that E_2^0 is sufficiently cathodic to E_1^0 so as the $I\Psi$ pattern decomposes into two independent waves*.

When $E \gg E_2^0$

$$I\Psi = I\Psi_1 = \{1 + \exp(nF/RT)(E - E_1^0)\}^{-1}$$

i.e. a standard n-electron wave corresponding to the standard potential E_1^0.

When $E \gg E_1^0$

$$I\Psi = 1 + I\Psi_2 = 1 + \{1 + \exp(nF/RT)(E - E_2^0)\}^{-1}$$

$I\Psi_2$ is thus a second wave added to the plateau of the first one corresponding to n electrons and the standard potential E_2^0. This is represented on Fig. 2 in dimensionless as well as in dimensioned scales. The straight lines corresponding to the logarithmic analysis of each wave are also shown on the Figure. The slope in each case is RT/nF (59.1/n mV at 25°C when decimal logarithms are used).

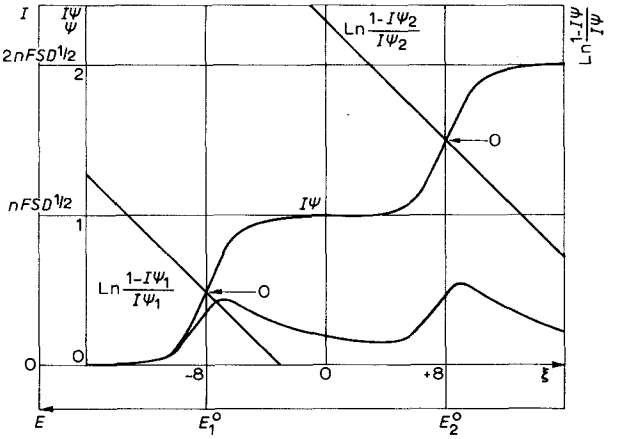

Fig. 2. Current, convoluted current and logarithmic analysis for two successive nernstian waves ($E_1^0 - E_2^0 = 400/n$ mV at 25°C).

The same kind of analysis is also applicable to successive waves arising from a mixture of reversibly reducible depolarizers.

The advantage of CPSV over LSV as regards successive waves lies in the fact that each wave can now be easily measured from the plateau of the preceding one as in polarography. Tedious reconstruction procedures from the ideal extension of the preceding wave[4,5] are thus avoided.

As noted before[6], the same polarization pattern would be obtained if fast

* The case of closely spaced and fused waves will be treated in a forthcoming publication.

electron transfer in solution such as:

$$A + C \rightleftharpoons 2B$$

occurred. Such a reaction scheme cannot therefore be distinguished from the present one with CPSV or any other electrochemical technique.

SECONDARY HOMOGENEOUS CHEMICAL REACTIONS

The following basic reaction schemes are successively considered: antecedent or consecutive first order reaction, consecutive dimerization, ECE and disproportionation processes. In each case "pure kinetic" conditions are assumed, *i.e.* a stationary state resulting from mutual compensation of diffusion and chemical reaction is established as regards the reacting particle.

The reaction scheme involving a first order reaction parallel to the electron transfer process is not considered here. Indeed, under "pure kinetic" conditions the LSV curve is an S-shape wave the $E_{\frac{1}{2}}$ of which is the standard potential of the redox couple[7,8]. It follows that the convoluted curve would be more difficult to analyze than the starting i–E wave. Here logarithmic analysis is better performed on the i–E wave itself.

Antecedent first order reaction (1)

$$A \underset{k_b}{\overset{k_f}{\rightleftharpoons}} B \overset{ne}{\rightleftharpoons} C \text{ (standard potential: } E^0;\ K = k_f/k_b)$$

Under pure kinetic conditions an S-shape LSV wave is obtained[9] the equation of which is:

$$\Phi + I\Phi \exp(nF/RT)\{E - (E^0 - (RT/2nF)\ln k\theta)\} = 1 \tag{14}$$

where $\Phi = i/nFSC^0 D^{\frac{1}{2}} K k_b^{\frac{1}{2}}$.

With a linear sweep $\theta = RT/nFv$, but it is easily seen that the mathematical analysis[9] does not necessarily require a linear relationship between potential and time. It follows that eqn. (14) is valid for any kind of sweeping the only condition for θ being to have the dimension of time.

The convoluted current is given by:

$$I = \frac{1}{\pi^{\frac{1}{2}}} \int_0^t \frac{i}{(t-\upsilon)^{\frac{1}{2}}} \, d\upsilon = nFSC^0 D^{\frac{1}{2}} K k_b^{\frac{1}{2}} \theta^{\frac{1}{2}} I\Phi \tag{15}$$

As the potential becomes more and more cathodic $\Phi \rightarrow 1$ and the current tends toward a plateau the height of which is:

$$i_l = nFSC^0 D^{\frac{1}{2}} K k_b^{\frac{1}{2}} \tag{16}$$

On the contrary, $I\Phi$, and thus I, do not tend toward a limiting value but go on increasing as shown in Fig. 3 where Φ and $I\Phi$ are represented as functions of the electrode potential. However a logarithmic analysis is still feasible deriving from eqn. (14):

$$E = E^0 - (RT/2nF)\ln k_b\theta + (RT/nF)\ln\{(1-\Phi)/I\Phi\}$$

i.e., according to eqns. (15) and (16):

$$E = E^0 - (RT/2nF)\ln k_b + (RT/nF)\ln\{(i_l - i)/I\} \tag{17}$$

The resulting straight line is also shown in Fig. 3. The slope is RT/nF (*i.e.* 59.1/n mV at 25° when using decimal instead of naperian logarithms). It is seen from eqn. (17) that a variation of the sweep rate does not alter the linearity nor change the position of the logarithmic analysis pattern.

Consecutive first order reaction (II)

$$A + ne \rightleftharpoons B \qquad \text{(standard potential } E^0\text{)}$$

$$B \xrightarrow{k} \text{products}$$

From the previous analysis[10] of the problem in LSV it follows that the equation of the wave is:

$$\Psi \exp(nF/RT)\{E-(E^0+(RT/2nF)\ln k\theta)\} = 1 - I\Psi \tag{18}$$

Ψ and $I\Psi$ are represented as functions of the electrode potential on Fig. 4, together

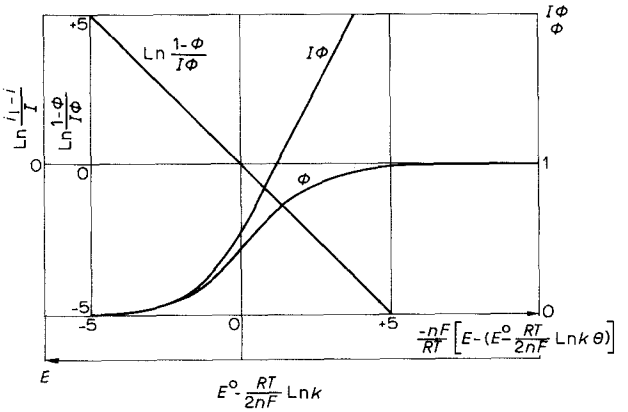

Fig. 3. Current, convoluted current and logarithmic analysis in the case of a first order antecedent chemical reaction.

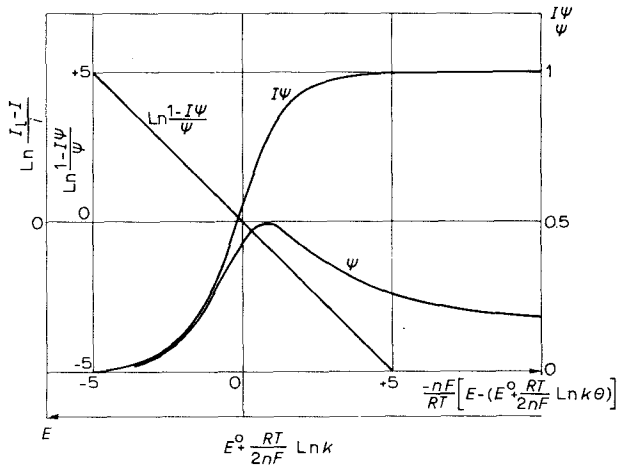

Fig. 4. Current, convoluted current and logarithmic analysis in the case of a consecutive first order chemical reaction.

with the logarithmic analysis of the $I\Psi$–E wave:

$$E = E^0 + (RT/2nF) \ln k\theta + (RT/nF) \ln \{1 - I\Psi)/\Psi\}$$

i.e., in dimensioned form:

$$E = E^0 + (RT/2nF) \ln k + (RT/nF) \ln \{(I_l - I)/i\}$$

Here again, as in the pure diffusion control case:

$$I_l = nFSC^0 D^{\frac{1}{2}} \tag{19}$$

The logarithmic straight line has still a slope of RT/nF (59.1/n mV at 25° for decimal logarithms). Its linearity and its location on the potential axis do not depend on the sweep rate.

Consecutive dimerization (III)

$$A + ne \rightleftharpoons B \qquad \text{(standard potential: } E^0\text{)}$$

$$2B \xrightarrow{k} \text{products}$$

From the analysis of the LSV wave[10] it follows that:

$$\Psi^{\frac{2}{3}} \exp(nF/RT)\{E - (E^0 + (RT/3nF) \ln \tfrac{2}{3}kC^0\theta)\} = 1 - I\Psi \tag{20}$$

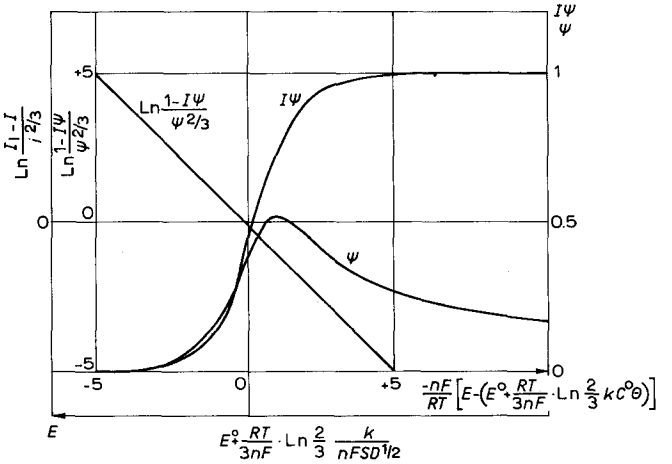

Fig. 5. Current, convoluted current and logarithmic analysis in the case of a consecutive dimerization.

Ψ and $I\Psi$ are represented on Fig. 5. Here again, the height of each point of the I–E wave is independent of the sweep rate and proportional to the initial concentration. The plateau value I_l is the same as given by eqn. (19). The logarithmic analysis of the wave:

$$E = E^0 + (RT/3nF) \ln \tfrac{2}{3}kC^0\theta + (RT/nF) \ln \{(1 - I\Psi)/\Psi^{\frac{2}{3}}\}$$

i.e.

$$E = E^0 + (RT/3nF) \ln \tfrac{2}{3}(k/nFSD^{\frac{1}{2}}) + (RT/nF) \ln \{(I_l - I)/i^{\frac{2}{3}}\}$$

leads to a straight line with the same slope as above which is independent of both sweep rate and initial concentration.

Other types of dimerization reaction schemes have been recently discussed involving coupling steps by attack on the substrate, electrode and solution electron transfers and protonation reactions[11,12]. The logarithmic analysis to be performed for each particular reaction mechanism can be readily derived from the LSV wave equations given in refs. 11, 12 (see Table 2 in ref. 11 and Table 3 in ref. 12).

ECE and disproportionation

(1) $A + ne \rightleftharpoons B$ (standard potential: E^0)

(2) $B \underset{k_f}{\overset{k_b}{\rightleftharpoons}} C$ ($k = k_f + k_b$, $K = k_f/k_b$ = equilibrium constant)

(3) $C + ne \rightarrow D$ (standard potential infinitely anodic to E^0)

(4) $B + C \xrightarrow{k_d} A + D$

It has been shown in the analysis of this reaction scheme[13–15] that the most typical situations with respect to mechanism diagnosis are met in three cases:
ECE mechanism: reaction (4) negligible, r.d.s.: reaction (2).
DISP1 mechanism: reaction (3) negligible, r.d.s.: reaction (2).
DISP2 mechanism: reaction (3) negligible, r.d.s.: reaction (4).

ECE (IV)

In "pure kinetic" conditions:

$$\tfrac{1}{2}\Psi \exp(nF/RT)\{E-(E^0+(RT/2nF)\ln k\theta/(1+K)^2)\} = 1-\tfrac{1}{2}I\Psi \qquad (21)$$

Comparing eqns. (18) and (21), it is seen that Ψ and $I\Psi$ have the same shape as in the case of a first order reaction following the charge transfer and are simply double in height. The same is true for i and I. Ψ and $I\Psi$ are thus represented on Fig. 4 making allowance for a reduction of the vertical scale by a factor of 2. The limiting value of I is now:

$$I_l = 2nFSC^0D^{\frac{1}{2}} \qquad (22)$$

The logarithmic analysis of the I–E wave now results in:

$$E = E^0 + (RT/2nF)\ln\{k/(1+K)^2\} + (RT/nF)\ln\{I_l - I)/i\}$$

the characteristics of which are the same as for reaction scheme (II) (Fig. 4).

DISP 1 (V)

Under "pure kinetic" conditions the LSV wave is the same as for the ECE case with a slight modification of the kinetic factor[15]. Thus:

$$E = E^0 + (RT/2nF)\ln\{k/2(1+K)\} + (RT/nF)\ln\{(I_l - I)/i\}$$

DISP 2 (VI)

From previous analysis of the LSV wave[13], it follows that:

$$(\tfrac{1}{2}\Psi)^{\frac{2}{3}} \exp(nF/RT)\{E-(E^0+(RT/3nF)\ln(k_d C^0\theta/3K)\} = 1-\tfrac{1}{2}I\Psi \qquad (23)$$

It then follows from comparison of eqns. (20) and (23) that Ψ and $I\Psi$ have

the same shape as in the case of consecutive dimerization (III) and are double in height. So are i and I. Figure 5 thus provides a representation of Ψ and $I\Psi$ making allowance for a reduction of the vertical scale by a factor of 2. The limiting value I_l is again given by eqn. (22). The logarithmic analysis of the I–E wave is then given by:

$$E = E^0 + (RT/3nF) \ln k_d/6KnFSD^{\frac{1}{2}} + (RT/nF) \ln \{(I_l - I)/i^{\frac{2}{3}}\}$$

the characteristics of which are strictly the same as for reaction scheme (III) (Fig. 5).

TABLE 1

CHEMICAL POLARIZATION—LOGARITHMIC ANALYSIS

Reaction scheme		*Logarithmic analysis (naperian logarithms)*
Pure diffusion control $A + ne \underset{(E^0)}{\rightleftharpoons} B$		$E = E^0 + \frac{RT}{nF} \ln \frac{I_l - I}{I}$
Antecedent first order reaction $A \underset{k_b}{\overset{k_f}{\rightleftharpoons}} B$ $\quad (K)$ $\quad B + ne \underset{(E^0)}{\rightleftharpoons} C$		$E = E^0 - \frac{RT}{2nF} \ln k_b + \frac{RT}{nF} \ln \frac{i_l - i}{I}$
Consecutive first order reaction $A + ne \underset{(E^0)}{\rightleftharpoons} B$ $\quad B \underset{k}{\longrightarrow}$ products		$E = E^0 + \frac{RT}{2nF} \ln k + \frac{RT}{nF} \ln \frac{I_l - I}{i}$
Consecutive dimerization $A + ne \underset{(E^0)}{\rightleftharpoons} B$ $\quad 2B \underset{k}{\longrightarrow}$ products		$E = E^0 + \frac{RT}{3nF} \ln \frac{2}{3} \frac{k}{nFSD^{\frac{1}{2}}} + \frac{RT}{nF} \ln \frac{I_l - I}{i^{\frac{2}{3}}}$
ECE and disproportionation (1) $A + ne \underset{(E^0)}{\rightleftharpoons} B$ (2) $B \underset{k_b}{\overset{k_f}{\rightleftharpoons}} C$ $\quad (K)$	ECE (3) $C + ne \rightarrow D$	$E = E^0 + \frac{RT}{2nF} \ln \frac{k}{(1+K)^2} + \frac{RT}{nF} \ln \frac{I_l - I}{i}$
	DISP1 (4) $B + C \overset{k_d}{\longrightarrow} A + D$ r.d.s.: (2)	$E = E^0 + \frac{RT}{2nF} \ln \frac{k}{2(1+K)} + \frac{RT}{nF} \ln \frac{I_l - I}{i}$
	DISP2 (4) $B + C \overset{k_d}{\longrightarrow} A + D$ r.d.s.: (4)	$E = E^0 + \frac{RT}{3nF} \ln \frac{k_d}{6\,KnFSD^{\frac{1}{2}}} + \frac{RT}{nF} \ln \frac{I_l - I}{i^{\frac{2}{3}}}$

The logarithmic analyses pertaining to each reaction scheme are summarized in Table 1. It is seen that the slope is RT/nF (*i.e.* $59.1/n$ mV at 25° when using decimal logarithms) in all cases. Also the location of the straight line along the potential axis is independent of both sweep rate and initial concentration in every case. This could appear in contradiction to the behaviour of the peak potential in LSV the variations of which, with the sweep rate and initial concentration, serve as diagnostic criteria in mechanism analysis. In fact this is only apparent and derives

from the fact that i and I do not have the same dimensions and do not vary in the same way with the sweep rate. For second order kinetics the introduction of ratios such as $I/i^{\frac{2}{3}}$ where both I and i are proportional to the initial concentration accounts for the influence of this factor.

It follows that changing the sweep rate, and for second order kinetics the initial concentration, results in the superimposition of all the resulting straight lines if the logarithmic analysis pertaining to the proper mechanism has been performed. This superimposition is the equivalent in each case of the variation of the LSV peak potential with v (and C^0). It must be emphasized that an actual improvement in accuracy over the peak potential method will be arrived at only if both operations are performed: checking the linearity of the logarithmic plot for each value of v (and C^0) and checking that the same plot is obtained for all the v (and C^0) values.

Another important role of the sweep rate is as follows. If the chemical de-activation process is not too fast, increasing the sweep rate will shift the system from "pure kinetic" conditions to pure diffusion control, where for fast charge transfer eqn. (10) will be applicable. From this fast sweep logarithmic analysis the standard potential E^0 can be deduced and then, turning back to the slow sweep experiments, the rate constant of the chemical steps can be determined from the value of the potential where the logarithmic term is zero using the formulas of Table I.

Between these two limiting behaviours there exists a range of sweep rates where the I–E wave possesses mixed character and fits neither the logarithmic analysis for "pure kinetic" conditions nor that of pure diffusion control. For a given sweep rate in this range the tendency is that the diffusion control analysis is followed at the foot of the wave and the "pure kinetic" analysis near the top of the wave so that information can nevertheless be gained from this intermediary type of wave. For second order kinetics, a decrease of the initial concentration, although performable in a more restricted range in practice, has the same effect as an increase of the sweep rate.

CHARGE TRANSFER KINETICS

The use of the I–E curves instead of the i–E curves allows a significant simplification of the use of LSV in studies on charge transfer kinetics. Indeed, the rate-potential law does not need to be known before the treatment of data but is obtained as a result of this treatment.

Since $(C_A)_0 \rightarrow 0$ as $E \rightarrow -\infty$, the I–E curve tends toward a plateau, the height of which is given by eqn. (9) regardless of the degree of reversibility of the charge transfer process.

Slow charge transfer: $A + n\,e \rightarrow B$

$$i = nFSk(E)(C_A)_0$$

It follows from eqns. (9) and (11) that:

$$k(E) = D_A^{\frac{1}{2}}\, i/(I_l - I)$$

The rate-potential relationship is thus readily obtained once the diffusion coefficient is known.

In the case where the rate law can be expressed in the Volmerian classical form:

$$k(E) = k_f^0 \exp(-\alpha nFE/RT)$$

the following logarithmic analysis:

$$E = (RT/\alpha nF) \ln (k_f^0/D_A^{\frac{1}{2}}) + (RT/\alpha nF) \ln [(I_l - I)/i]$$

gives rise to a straight line. The transfer coefficient α can be derived from the slope: $RT/\alpha nF$ ($59.2/\alpha n$ at 25°C with decimal logarithms) and the rate constant k_f^0 from the intercept. Here again, repetition of the experiment at various sweep rates, increases the certainty in mechanism diagnosis and the accuracy in the determination of α and k_f^0.

"Quasi-reversible" charge transfer: $A + ne \rightleftharpoons B$

$$i = nFSk(E) \{(C_A)_0 - (C_B)_0 \exp(nF/RT)(E - E^0)\}$$

It follows from eqns. (9), (11) and (12) that:

$$k(E) = D_A^{\frac{1}{2}} \frac{i}{I_l - I\{1 + \exp(nF/RT)(E - E_{\frac{1}{2}})\}}$$

This requires the half wave potential of the purely diffusion controlled wave $E_{\frac{1}{2}}$ to be known. This situation can be met by decreasing the sweep rate if the charge transfer is not too slow in respect of the available sweep rate range. In this condition $E_{\frac{1}{2}}$ derives from a logarithmic analysis such as described by eqn. (10) and in the first line of Table 1.

If a Volmer-type relationship exists the following logarithmic analysis:

$$E = \frac{RT}{\alpha nF} \ln \frac{k_f^0}{D_A^{\frac{1}{2}}} + \frac{RT}{\alpha nF} \ln \frac{I_l - I\{1 + \exp(nF/RT)(E - E_{\frac{1}{2}})\}}{i}$$

gives rise to a straight line. Again the transfer coefficient can be derived from the slope and the rate parameter from the intercept. When the transfer rate increases the term $I_l - I\{1 + \exp(nF/RT)(E - E_{\frac{1}{2}})\}$ becomes smaller and smaller and thus the accuracy in the determination of α and k_f^0 diminishes accordingly. The performances in this connection are related to the practical availability of high sweep rates.

Correction for the double layer effect

In the case where the diffusion layer thickness is large with respect of that of the double layer[16] the correction for the double layer effect is greatly simplified in comparison with LSV[17]: no particular relationship, such as a linear one[17], between the potential of the outer Helmholtz plane ϕ_2 and the input potential E is required in order to treat the data. This derives again from the fact that $k(E)$ need not be known *a priori*. In the present case $k(E)$ contains the double layer effect which can then be corrected for *a posteriori* using the experimental dependence of ϕ_2 on E.

For example, in the case of a slow charge transfer exhibiting a Volmerian behaviour:

$$i = nFS(C_A)_0 k_f^0 \exp(\alpha n - z)F\phi_2/RT \exp(-(\alpha nFE/RT))$$

(z is the charge number of the species A).

The logarithmic analysis:

$$E = \left(1 - \frac{z}{\alpha n}\right)\phi_2 + \frac{RT}{\alpha nF} \ln \frac{k_f^0}{D_A^{\frac{1}{2}}} + \frac{RT}{\alpha nF} \ln \frac{I_l - I}{i}$$

leads to α and k_f^0: once $\phi_2(E)$ is known, α can be determined through an iteration procedure. Knowing α, k_f^0 is readily determined from the intercept of the logarithmic plots.

SPHERICITY EFFECTS

When a mercury drop is used as working electrode, diffusion is approximately spherical. In these conditions, the dimensionless current Ψ (eqn. 2) for a diffusion controlled system is expressed by[18]:

$$\Psi = \Psi_{lin} + \sigma/\{1 + \exp(-\xi)\} \tag{24}$$

where ξ is defined by eqn. (7), Ψ_{lin} is the dimensionless current for linear diffusion and σ the sphericity parameter:

$$\sigma = \frac{1}{r_0} D_A^{\frac{1}{2}} \theta^{\frac{1}{2}} \left(= \frac{1}{r_0} D_A^{\frac{1}{2}} \left(\frac{RT}{nFv}\right)^{\frac{1}{2}} \text{ in LSV} \right) \tag{25}$$

(r_0 = drop radius)

Equation (24) derives from the Laplace equation:

$$\overline{b_0} = \overline{\Psi}/(s^{\frac{1}{2}} + \sigma) \tag{26}$$

It follows that:

$$I\Psi = \frac{1}{1 + \exp(-\xi)} + \sigma \int_{-u}^{\xi} \frac{1}{1 + \exp(-\eta)} \frac{d\eta}{(\xi - \eta)^{\frac{1}{2}}} \tag{27}$$

($-u = (nF/RT)(E_i - E_{\frac{1}{2}})$ is the dimensionless expression of the starting potential of the scan.)

Equation (27) has been numerically computed for various values of the parameter σ (the FORTRAN program for an 1130 IBM computer is available on request). As an example the $I\Psi$–ξ curve is compared to the corresponding linear diffusion curve on Fig. 6 for $\sigma = 0.02$. On the same Figure the standard logarithmic analysis (eqn. 8) of the linear diffusion curve is compared to the logarithmic analysis: $\ln\{I\Psi(10) - I\Psi\}/I\Psi$ of the spherical diffusion wave. It is seen that $I\Psi$ does not reach a plateau but increases slowly in a roughly linear way as the potential becomes more and more negative. The error on the plateau current reaches 7% for $E_{\frac{1}{2}} - E = 256/n$ mV and 4% for $E_{\frac{1}{2}} - E = 128/n$ mV at 25°. Similarly the deviation from linearity of the logarithmic plot beyond the half-wave potential is not negligible. If one considers that:

$$r_0 = 0.2 \text{ mm}, \quad n = 1, \quad D_A = 10^{-5} \text{ cm s}^{-1}, \quad T = 298°\text{K},$$

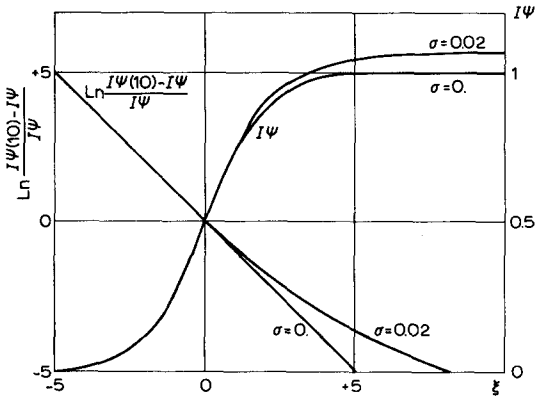

Fig. 6. Convoluted waves and logarithmic analysis for spherical and linear diffusion.

the effect of sphericity reaches the magnitude shown on Fig. 6 as soon as the sweep rate becomes smaller than 1.6 V s^{-1}. In LSV for similar conditions the error on the peak height would be 3.5% and about 1 mV on the peak potential. CPSV is thus significantly more sensitive to sphericity effects than the peak potential method in LSV.

It is therefore desirable to devise a procedure for data processing that takes this effect into account. However the most useful conditions to consider are those where the magnitude of the sphericity effect is small. A reason for this is that the diffusion is not accurately spherical owing to shielding by the capillary tip. On the other hand, the sphericity effect decreases as the sweep rate is raised (eqn. 25) and too small sweep rates cannot be used owing to the possible interference of natural convection.

In conditions where the magnitude of the sphericity effect is small a simple correction procedure can be proposed:

when $\sigma \rightarrow 0$ eqn. (26) becomes:

$$\overline{b_0} = \overline{\Psi}/s^{\frac{1}{2}} - \sigma\overline{\Psi}/s$$

and then:

$$I\Psi = \frac{1}{1+\exp(-\xi)} + \sigma\int_0^\tau \Psi \, d\upsilon$$

i.e.

$$I = I_{lin} + (D_A^{\frac{1}{2}}/r_0)\int_0^t i \, d\upsilon \qquad (28)$$

As the electrode potential is made more and more negative I_{lin} tends toward a limiting value $I_{lin,1}$ (eqn. 9) and thus I becomes a linear function of the integral in the right-hand part of eqn. (28). Thus this integral will be calculated from the i–E curve together with I. Then I will be plotted against the integral. The slope of the linear dependence reached at negative values of the electrode potential will provide σ. σ being known, the I_{lin} can be computed point by point from eqn. (28).

Performing the correction for sphericity effect, care must be exercized as to the selection of the base line from which the values of the current i are measured.

Indeed, let us suppose that the base line is horizontal and is in error by an amount called A. Then the apparent values of I, designated I_{ap} will be:

$$I_{ap} = I + \frac{2A}{\pi^{\frac{1}{2}}} t^{\frac{1}{2}} = I + \frac{2A}{\pi^{\frac{1}{2}}} \left(\frac{RT}{nF} \frac{E_i - E}{v} \right)^{\frac{1}{2}}$$

The resulting effect is thus the addition, or the subtraction according to the sign of A, of a parabola the top of which is located at the starting potential of the scan. For negative potentials this can result in a roughly linear increase or decrease of the plateau, leading to an overestimation or underestimation of the sphericity correction.

CORRECTION FOR OHMIC DROP

The effect of the uncompensated resistance R_u remaining between the working electrode and the reference electrode on the potential difference E' across the faradaic impedance is given by:

$$E' = E + R_u i$$

where $E = E_i - vt$ is the applied potential and i the current flowing through the working electrode.

In conditions where the double layer charging current is small with respect to the faradaic current, *i.e.* for moderately high sweep rates, this is the only effect of R_u on the polarization curves[19].

As concerns CPSV it follows that the correction for the ohmic drop consists simply in plotting the convolution integral I and the logarithmic analysis function against E' instead of E. This is readily performable once R_u has been measured[20] since i is known for every point of the $I(E)$ curve.

The procedure is applicable regardless of the mechanism of the faradaic process. This is a significant advantage of CPSV over LSV since in the last case the correction procedure depends on the particular mechanism considered[1,21–24] and involves the use of working curves in each case except for small ohmic drops where linearized corrections can be used[19,24].

EXPERIMENTAL

We present here an experimental example of the study of a single diffusion controlled wave and of two successive diffusion controlled waves with corrections for the sphericity effect and for ohmic drop. In both cases the experimental system studied is the reduction on a mercury drop of a 1 mM l^{-1} solution of *meta*-dinitrobenzene in dimethylformamide with 0.1 M l^{-1} tetraethylammonium perchlorate as supporting electrolyte.

Chemicals

All chemicals were reagent grade and were used without further purification (*meta*-dinitrobenzene: Hopkin and Williams, pure grade; tetraethylammonium perchlorate: Carlo Erba, polarographic grade; DMF: Carlo Erba, Spectro grade).

Apparatus and measuring procedures

The cell and electrodes were as already described[10], and similarly the oscilloscope, the function generator and the synchronisation of the drop with the applied voltage. The potentiostat was a solid state operational amplifier device with provision for compensation of the cell resistance by a variable positive feedback[20].

The conversion of the analogue i–t signal into a digital form was performed with a DIDAC 800 Intertechnique apparatus. The accuracy is 0.5% full scale and the shortest time of conversion 20 μs. Each i–t curve was digitalized into 200 points. The digitalized signal is collected at the output under the form of punched tapes. These are put into an IBM 1130 computer and computed by means of FORTRAN programs corresponding to the calculation of I, the correction for sphericity effects, the correction for ohmic drop and the logarithmic analysis as described above.

For routine use of CPSV it would be desirable to have a simpler on-line apparatus just able to perform the strictly necessary operations. However in a preliminary research stage the system we used offers more versatility.

Results

Figure 7 shows the results of each transformation for the first wave of *meta*-dinitrobenzene, starting from the i–E digitalized curve: calculation of I (E), correction for sphericity and logarithmic analysis without correction for ohmic drop. This leads to a straight line the slope of which (64 mV) is not exactly the predicted one. The second straight line was obtained by plotting the logarithmic function against $E' = E + R_u i$ instead of E ($R_u = 370\ \Omega$ as measured by an already described procedure[20]). Now the value of the slope is quite correct.

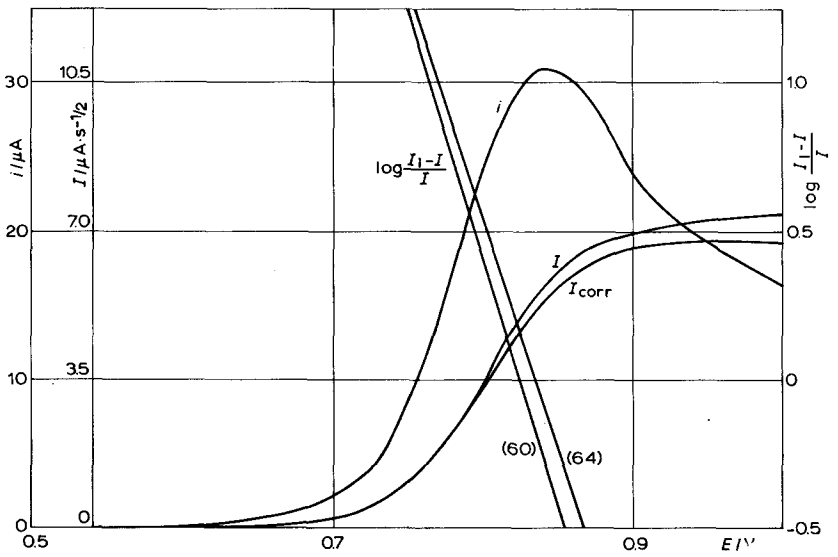

Fig. 7. Convolution and logarithmic analysis of the first wave of *meta*-dinitrobenzene in DMF, I_{corrs} = convoluted current corrected for sphericity. The logarithmic analyses are represented with (60) and without (64) correction for ohmic drop.

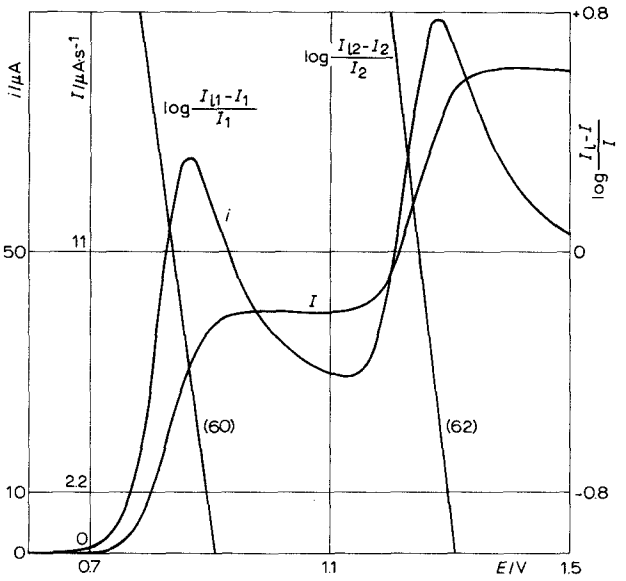

Fig. 8. Convolution and logarithmic analysis of the two waves of *meta*-dinitrobenzene in DMF (the curves are corrected for sphericity and ohmic drop).

Figure 8 shows the original i–E curve for both waves and the results of the computation of the I–E curve after correction for sphericity effects. The two straight lines represent the logarithmic analysis of each wave after correction for ohmic drop. The slope for the second wave is very slightly larger than the expected value.

ACKNOWLEDGEMENTS

Work was supported in part by the C.N.R.S. (Equipe de Recherche Associée no. 309: "Electrochimie Organique"). Prof. M. Hulin, Université de Paris VI is thanked for the permission of using the 1130 IBM computer of the "Groupe de Physique des Solides, Ecole Normale Supérieure, Paris".

SUMMARY

Starting from digitalized polarization curves, a new method is proposed for processing the data obtained by linear sweep voltammetry (LSV). This method, termed Convolution Potential Sweep Voltammetry (CPSV) consists in calculating directly from the experimental data the convolution integral of the current–time function with the function $t^{-\frac{1}{2}}$. The formal kinetics of the basic reaction schemes involving rate determining chemical reactions or charge transfers is performed. Correction procedures for sphericity effects and ohmic drop are proposed. The applicability of the method is illustrated using the reduction of *meta*-dinitrobenzene in DMF as example.

It is shown that the main advantages of CPSV over LSV are: (*a*) simplification of the mechanistic analysis when secondary chemical reactions are involved, (*b*) analysis of the charge transfer kinetics and correction of double layer effects without knowing *a priori* the form of the rate–potential relationship, (*c*) improvement in accuracy owing to the use of all the information contained in the polarization curve and not only in the peak values, (*d*) significant simplification of the correction for ohmic drop.

REFERENCES

1 C. P. Andrieux, L. Nadjo and J. M. Savéant, *J. Electroanal. Chem.*, 26 (1970) 147.
2 K. B. Oldham, *Anal. Chem.*, 44 (1972) 196.
3 M. Grenness and K. B. Oldham, *Anal. Chem.*, 44 (1972) 1121.
4 D. S. Polcyn and I. Shain, *Anal. Chem.*, 38 (1966) 370.
5 S. P. Perone, J. W. Frazer and A. Kray, *Anal. Chem.*, 43 (1971) 1485.
6 C. N. Andrieux and J. M. Savéant, *J. Electroanal. Chem.*, 38 (1970) 339.
7 J. M. Savéant and E. Vianello in Longmuir (Ed.), *Advances in Polarography*, 1960, t. 2, p. 367.
8 J. M. Savéant and E. Vianello, *Electrochim. Acta*, 10 (1965) 905.
9 J. M. Savéant and E. Vianello, *Electrochim. Acta*, 8 (1963) 905.
10 J. M. Savéant and E. Vianello, *C.R.*, 256 (1963) 2597.
11 C. P. Andrieux, L. Nadjo and J. M. Savéant, *J. Electroanal. Chem.*, 42 (1973) 223.
12 L. Nadjo and J. M. Savéant, *J. Electroanal. Chem.*, in press.
13 M. Mastragostino, L. Nadjo and J. M. Savéant, *Electrochim. Acta*, 13 (1968) 721.
14 S. W. Feldberg, *J. Phys. Chem.*, 73 (1969) 1238.
15 L. Nadjo and J. M. Savéant, *J. Electroanal. Chem.*, 33 (1971) 419.
16 H. Matsuda and P. Delahay, *J. Phys. Chem.*, 64 (1960) 322.
17 M. Caselli, G. Ottombrini and P. Papoff, *Electrochim. Acta*, 13 (1968) 241.
18 W. H. Reinmuth, *J. Amer. Chem. Soc.*, 79 (1957) 6358.
19 J. C. Imbeaux and J. M. Savéant, *J. Electroanal. Chem.*, 28 (1970) 325.
20 D. Garreau and J. M. Savéant, *J. Electroanal. Chem.*, 35 (1972) 309.
21 R. S. Nicholson, *Anal. Chem.*, 37 (1965) 667.
22 W. T. De Vries and E. Van Dalen, *J. Electroanal. Chem.*, 10 (1965) 183.
23 S. Roffia and E. Lavachielli, *J. Electroanal. Chem.*, 22 (1969) 117.
24 J. C. Imbeaux and J. M. Savéant, *J. Electroanal. Chem.*, 31 (1971) 183.